JOURNAL OF DEGRADED AND MINING LANDS MANAGEMENT
ISSN: 2339-076X (p); 2502-2458 (e), Volume 6, Number 2 (January 2019):1675-1696
DOI:10.15243/jdmlm.2019.062.1675

Research Article

Improving the accuracy and reliability of land use/land cover simulation by the integration of Markov cellular automata and landform-based models – a case study in the upstream Citarum watershed, West Java, Indonesia

Fajar Yulianto*, Suwarsono, Sayidah Sulma

Remote Sensing Application Center, Indonesian National Institute of Aeronautics and Space (LAPAN), Jl. Kalisari No. 8, Pekayon, Pasar Rebo, Jakarta 13710, Indonesia

*corresponding author: fajar.lapan.rs@gmail.com, fajar.yulianto@lapan.go.id

Received 30 November 2018, Accepted 27 December 2018

Abstract: Land use/land cover (LULC) is one of the important variables affecting human life and the physical environment. Modelling of change in LULC is an important tool for environmental management and for supporting spatial planning in environmentally important areas. In this study, a new approach was proposed to improve the accuracy and reliability of LULC simulation by integrating Markov cellular automata (Markov-CA) and landform-based models. Landform characteristics, positions and patterns influence LULC changes that are important in understanding the effects of environmental change and other physical factors. The results of this study showed that integration of Markov-CA and landform-based models increased correct rejection as a component of agreement and reduced incorrect hits and false alarms as components of disagreement for the percentage of the study area in each resolution (multiple of native pixel size). Correctly simulated hits as a component of agreement change also increased, even though nine of the 18 pairs of three-map comparisons showed a decline in this aspect. Meanwhile, misses as a component of disagreement change simulated as persistence also increased, although six of the 18 pairs of data showed a decline. Based on the overall three-map comparison analysis, there was an increase in the figure of merit (FOM) values after the Markov-CA and landform-based models were integrated, although six of the 18 pairs of data indicated a decrease in FOM values. This indicates improved results after integration of Markov-CA and landform-based models.

***Keywords**: Citarum watershed, Indonesia, landform-based model, Markov-CA, remote sensing*

To cite this article: Yulianto, F., Suwarsono, and Sulma, S. 2019. Improving the accuracy and reliability of land use/land cover simulation by the integration of Markov cellular automata and landform-based models - a case study in the upstream Citarum watershed, West Java, Indonesia. J. Degrade. Min. Land Manage. 6(2): 1675-1696, DOI: 10.15243/jdmlm. 2019.062.1675.

Introduction

One of the fundamental and interrelated variables that affect the human and physical environment is LULC. LULC has an influence on the ecosystem and also on global environmental and human influences related to climate change (Vitousek, 1994; Skole, 1994; Penner, 1994; Chapin et al., 2000; Foody, 2002; Foley et al., 2005; Verburg, 2009). LULC change models are important tools for the integration of environmental management and can be used to support causal analysis in respect to the dynamics of LULC change. In addition, the prediction of LULC is an important parameter for LULC policy and planning (Verburg et al., 2002; 2004).

To improve the accuracy and reliability of LULC simulations, several models using various approaches have been developed, such as neural-network-based CA models (Li and Yeh, 2002), multi-agent systems (Tian et al., 2011), the combined top-down system-dynamics model, the bottom-up cellular automata model and the artificial neural-network model (Wang et al., 2011), ant colony optimization, Markov chain and CA models (Yang et al., 2012), graphics processing units and CA models (Li et al., 2012), chi-squared automatic integration detection decision tree, Markov chain and CA models (Abubakr and Biswajeet, 2015), integration of landscape pattern indexes, Markov chain and CA (Yang et al., 2014) and others.

A new approach is proposed in this study to improve the accuracy and reliability of LULC simulation. The integration of Markov-CA and landform-based models were used to create LULC simulation. Landforms are defined as specific geomorphic features of the earth's surface that have a characteristic, recognizable shape and are formed by natural processes, such as plains, mountains, hills and valleys (Blaszczynski, 1997; Tagil and Jenness, 2008). Landform structures reflect the cumulative influences of geomorphic, geological, hydrological, ecological and soil-forming processes (MacMillan et al., 2000; MacMillan and Shary, 2009). The relationships between LULC and landform are strongly correlated and provide important keys to understanding the effects of environmental change and other physical aspects and important information to support the management of natural resources and the environment. In addition, the characteristics, positions and patterns of landforms as objects that exist on the surface of the earth can affect changes in LULC and can contribute to the formulation of environmental policy. LULC change models can be used as tools to support analysis of the causes and consequences of LULC change and the levels and spatial patterns of LULC change and to estimate its impact. Furthermore, modelling is useful for better understanding the functions of LULC systems and for supporting LULC planning and policies. In addition, it can be used to analyze changing LULC and thus to make more informed decisions (Blaszczynski, 1997; Brabyn, 1998; Tunçay et al., 2014).

An integration experiment between the Markov-CA and landform-based models was performed in this study to demonstrate the influence of landform in creating simulated future LULC. The case study area was chosen to create and demonstrate a novel LULC model in the upstream Citarum watershed, West Java, Indonesia.

Study area

A case study to demonstrate the feasibility of the integration of Markov-CA and landform-based models was undertaken by simulating LULC in the upstream Citarum watershed, West Java, Indonesia (Figure 1). The location was selected for this demonstration because of its varied landform types (including plains, hills, mountains and valleys) and the dynamics of different LULC changes (primary forest, secondary forest and mixed garden, plantation, wet agricultural land, dry land farming, built land, and water bodies) present in the area.

Materials and Methods

Data availability

LULC information for 1996, 2000, 2003 and 2009 taken from the study conducted by Yulianto et al. (2018) was used as the input data for this study. Multi-temporal Landsat images with a resolution of 30 m and at Level 1 Geometric (L1G) with sensor TM and ETM+ (path/row: 121/65 and 122/65) were used to derive the LULC information for the study. Seven classes of LULC were used: class 1: built land; class 2: primary forest; class 3: secondary forest and mixed garden; class 4: plantation; class 5: wet agricultural land; class 6: dryland farming; class 7: water body. These types of LULC were identified for this study based on the maximum likelihood classification approach (Table 1) (complete and detailed information is presented by Yulianto et al. (2018)).

Furthermore, Landsat 8 OLI/TIRS imagery was used as the input for LULC classifications in 2017 using the maximum likelihood approach. In this study, the LULC data for 1996, 2000 and 2003 were used as inputs to integrate experiments between the Markov-CA and landform-based models to demonstrate the influence of landform in changes to future LULC. Meanwhile, LULC data for 2009 and 2017 were used as the base reference to simulate LULC (Figure 2). Landsat 8 OLI/ TIRS images were provided by the Remote Sensing Technology and Data Center (LAPAN). The input data used to create the landform-based model was SRTM30 DEM, provided by the US Geological Survey (USGS). In addition, these data were also used for inputs in making potential map transitions (with elevation and slope parameters) and were then combined with topographic maps (with parameters of paths, rivers and others). The topographic map was provided by the Indonesian Geospatial Information Agency (BIG). Detail of the types of spatial data used in this study can be found in Table 2.

Markov-CA model

The Markov-CA model is the combination of Markov chain and cellular automata approach to simulate and predict LULC. A Markov chain is a stochastic model based on an evolutionary time trend that can describe the probability of object change from one class to another, e.g., dry land farming to built land (Thomas and Laurance, 2006; Behera et al., 2012). Meanwhile, a cellular automaton is an aspect of the geospatial elements that focuses on the variation and dynamics of object change. It can be used to simulate characteristics of spatial-temporal objects in a complex system which cannot be represented by a specific equation model (Mousivand et al., 2007; Arsanjani et al., 2013; Yang et al., 2014). There are three stages to the implementation of the Markov-CA model for simulating and predicting LULC: (a) calculate the transition area matrix of LULC; (b) create the potential transition map; and (c) simulate LULC using Markov-CA (Thomas and Laurence, 2006; Behera et al., 2012; Yang et al., 2014; Keshtkar and Voigt, 2016; Yulianto et al., 2016; 2018). In this study, the Markov-CA model for simulating and predicting LULC was processed by IDRISI Andes software, developed by Clark Labs at Clark University.

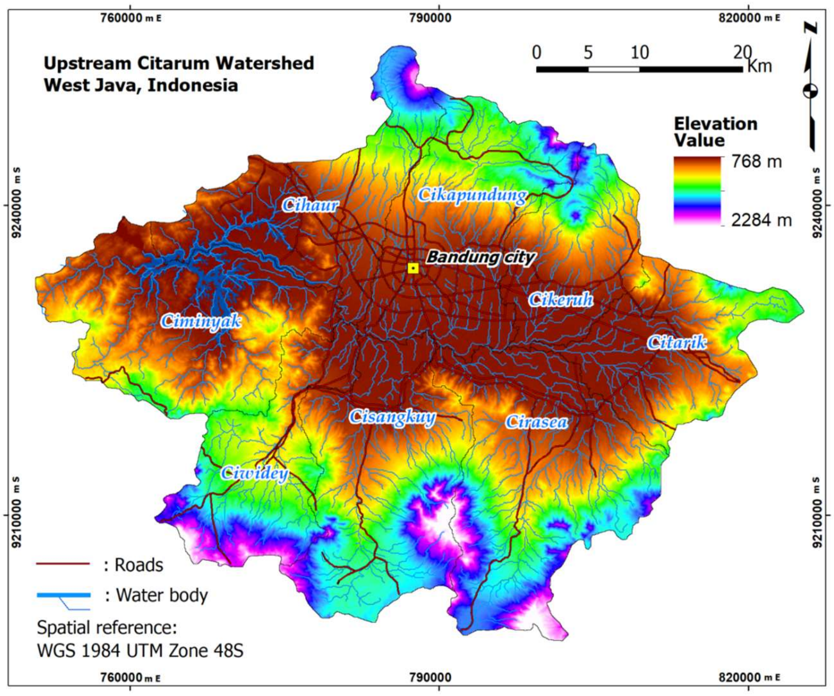

Figure 1. The location of the study area of upstream Citarum watershed, West Java, Indonesia

Table 1. LULC descriptions used in this study

Class	LULC type	Description
1	Built land	Consists of all residential, commercial and industrial areas, villages, settlements, transportation infrastructure and others.
2	Primary forest	Consists of natural forests that have not been disrupted by human exploitation.
3	Secondary forest and mixed garden	Consists of industrial plantation forests and some garden planting, coconuts, fruits and others.
4	Plantation	Consist of conservation land, tea plantations and others.
5	Wet agricultural land	Consists of land that requires much water for its planting pattern: irrigated rice fields, rice terraces and others.
6	Dryland farming	Consists of land that requires little water for its cropping pattern: fields, moorland and others.
7	Water body	Consists of all water sources, rivers, reservoirs, ponds and others.

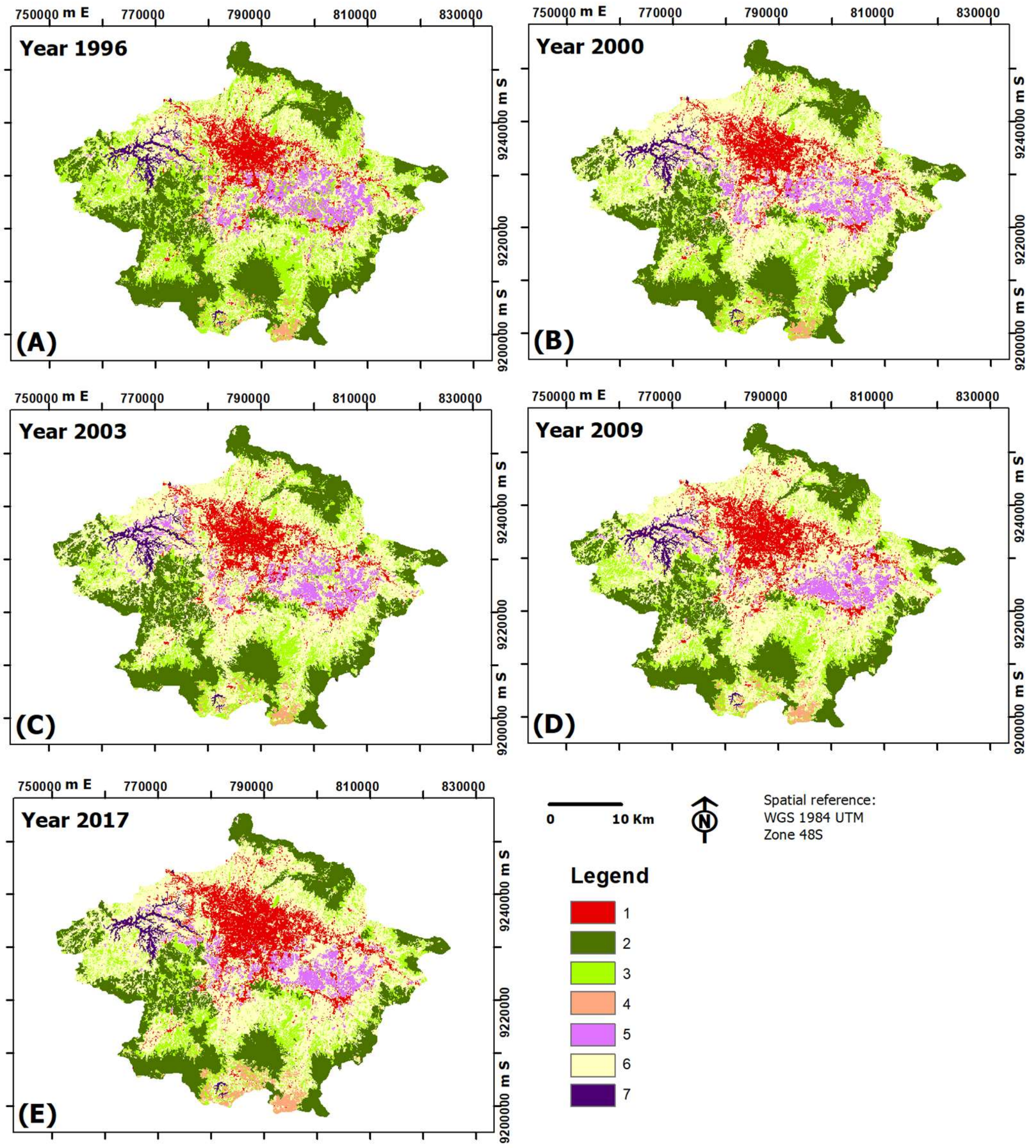

Figure 2. LULC maps used in this study: A) LULC in 1996; B) LULC in 2000; C) LULC in 2003; D) LULC in 2009; E) LULC in 2017. A), B) and C) were used as inputs to integrate experiments between the Markov-CA and landform-based models in this study. Meanwhile, D) and E) were used as base references to simulate LULC. Class 1: built land; class 2: primary forest; class 3: secondary forest and mixed garden; class 4: plantation; class 5: wet agricultural land; class 6: dryland farming; class 7: water body

Calculation of transition area matrix using the Markov chain

In the first stage, the transition area matrix of LULC from year (t) to ($t + i$) can be predicted by the Markov chain model, which is a raster-based spatial analysis. In this study, pairs of LULC maps for 1996, 2000 and 2003 were applied to calculate the transition area matrix used to simulate and predict LULC in 2009 and 2017, with a proportional error of 15%. According to Keshtkar and Voigt (2016), the results of matrix records show the number of pixels that are expected and estimate replacements from one class object to another in a specified period in the future and the trends observed in the past.

Generated transition potential map

The information provided by the transition potential map can be used to control for the spatial distribution of LULC. In the second stage, the transition potential map was generated by GIS.

There are three approaches used in GIS analysis: multi-criteria evaluation (MCE), analytical hierarchy process (AHP) and fuzzy membership functions. The MCE approach can be used to determine decision support in situations where a single decision maker is faced with many criteria usually not compatible and dependent on the decision of all decision makers. Furthermore, the weight calculation in the MCE approach is based on the AHP approach (Satty and Vargas, 2001).

Table 2. Types of spatial data used in this study

Data type	Acquisition date	Spatial resolution/ map scale	Explanation	Source
LULC in 1996	03 August 1996 and 25 July 1996	30 m	The result of Landsat 5 TM classification from Path/Row:121/65 and 122/65	Yulianto et al. (2018)
LULC in 2000	22 and 28 August 1990	30 m	The result of Landsat 7 ETM+ classification from Path/Row: 121/65 and 122/65	Yulianto et al. (2018)
LULC in 2003	09 and 16 August 2003	30 m	The result of Landsat 5 TM classification from Path/Row:121/65 and 122/65	Yulianto et al. (2018)
LULC in 2009	29 July and 07 August 2009	30 m	The result of Landsat 5 TM classification from Path/Row: 121/65 and 122/65	Yulianto et al. (2018)
Landsat 8 OLI/ TIRS	19 and 26 August 2017	30 m	Path/Row: 121/65 and 122/65	LAPAN
SRTM30 DEM	11 February 2000	30 m	-	USGS
Topographic map	1998	1:25,000	-	BIG

Table 3. Extracted weights based on MCE, AHP and fuzzy membership functions. Modified from Gemitzi et al. (2011), Keshtkar and Voigt (2016), and Shahabi et al. (2016)

Factor or parameter	Type of function	Control points	Weight
Elevation*	Sigmoidal	700–800 m (highest suitability) 800–1200 m (decreasing suitability) > 1200 m (no suitability)	0.16
Slope	Sigmoidal	< 3% (highest suitability) 3–15% (decreasing suitability) > 15% (no suitability)	0.18
Distance from the nearest road	J-shaped	< 500 m (highest suitability) 500–1000 m (decreasing suitability) > 1000 m (no suitability)	0.31
Distance from water body	Linear	> 1000 m (highest suitability) 200–1000 m (decreasing suitability) < 200 m (no suitability)	0.14
Distance from urban area	Linear	< 5 km (highest suitability) 5–10 km (decreasing suitability) > 10 km (no suitability)	0.21

* Elevation is calculated at an altitude of more than 700 m above sea level in the study area

The AHP approach, as part of MCE, was applied and used to determine the weights of the factors or parameters by means of pairwise assessments. A pairwise comparison matrix was created by assigning one row and one column for each factor (Mesgari et al., 2008). Meanwhile, fuzzy membership functions were used for standardization of factors or parameters, for realvalued functions whose value is between 0 and 1. The selection of a suitable membership function for the fuzzy set is one of the most important activities in fuzzy logic, it is the responsibility of the user to select the function that is the best representation for the fuzzy concept to be modelled (Mesgari et al., 2008; Oinam et al., 2014; Yeganeh and Sabri, 2014). In this study, the factors or parameters used to create the potential transition map were elevations, slope, distance from nearest roads, distance from water bodies and distance from urban areas.

Technically, the stages in determining the weights in this study were as follows: (a) create a standardization of parameters with values between 0 and 1 based on fuzzy membership functions; (b) the results of the standardization of parameters were then weighted using MCE to determine the weight that affects the trigger or inhibitor of LULC change in the study area; (c) determination of MCE to make the potential transition map, carried out based on the AHP approach by pairwise assessment from the comparison matrix. The results of extracted weights based on MCE, AHP and fuzzy membership functions can be found in Table 3, together with the control points used to limit suitability for each factor or parameter.

Simulated LULC using CA model

In the third stage, the prediction of LULC can be simulated and performed using the CA model (Yang et al., 2014; Keshtkar and Voigt, 2016; Yulianto et al., 2018). Furthermore, the results of the transition area matrix using Markov chain and the potential transition map were integrated into this model. According to Yang et al. (2014), the transition rule for the Markov-CA model is as presented in Equation 1:

$$if\ K_j = \max\ (K_1,\ K_2, K_3, \dots, K_n\ )\ and\ L_{i,j} < \frac{L_{i,j}}{T}\ then\ M_i \rightarrow\ M_j \quad \text{..................................} \ (1)$$

where K_j is the potential LULC transit to the LULC class j; $L_{i,j}$ is the total area from LULC class i to LULC class j in the current iteration; T is the time for the iteration; M_i is the LULC class i; M_j is the LULC class j.

Landform-based model

In the past, landform classification properties was measured by calculating their geometry manually. Recently, however, the use of computer technology for this process developed rapidly. New spatial analysis methods, the development of algorithms and the ease of obtaining digital elevation data have contributed to earth - oriented geomorphometrics (Horton, 1945; Miller, 1953; Coates, 1958; Chorley, 1972; Evans, 1972; Tagil and Jenness, 2008). Semi-automated landform-based classification is one of the efforts used to simplify and quickly process mapping and classification of landforms that was previously carried out manually. Several aspects of the relevant landform classification approach are developed and applied with semi-automatic classification (MacMillan and Shary, 2009). There are several methods and algorithms that can be used for automated landform-based classification, such as a curvature-based approach (Ramalingan et al., 2006), fuzzy landforms elements (Irvin et al., 1997; Burrough, 2000), pattern recognition (Jasiewicz and Stepinski, 2012), relief segmentation and object-based methods (Drăguţ and Eisank, 2012), morphometric features (Ehsani and Quiel, 2008), terrain clustering (Giguere and Dudek, 2009) and others.

Topographic position index (TPI) is the landform-based model approach used in this study, as proposed by Guisan et al. (1999), Weiss (2000), Wilson and Gallant (2000). TPI landform-based models can illustrate the difference between elevation value in a pixel cell and the average elevation of the neighbourhoods surrounding it. A positive value indicates that the pixel cell has a value higher than the neighbouring pixels, whereas a negative value indicates that the pixel cell has a value lower than the neighbouring pixels. TPI value provides power by which to classify landscapes and morphological classes (Weiss, 2005; Jenness, 2010; Mokarram and Sathyamoorthy, 2015). In detail, the definitions of landform classes using the TPI model can be found in Table 4 (Tagil and Jenness, 2008; Mokarram and Sathyamoorthy, 2015). Automated extraction of landform elements can be derived from SRTM30 DEM data to create landform-based classification with the TPI approach. System for Automated Geoscientific Analyses (SAGA) Ver 6.3 software was used in this study for automatic land elements from TPI extraction (www.saga-gis.org). The algorithm used to combine TPI value in various neighbourhood scenarios can be presented in Equation (2).

$$Prob\_total\ = \sum_{x=1}^{y} \frac{Prob\_value_{x(i,j)}}{y} \quad \text{..................} \ (2)$$

where $Prob\_total$ is the total of probability value for landform model. $Prob\_value_{x(i,j)}$ is the probability value in various neighbourhood scenario (x), (for $x = 1, 2, 3, \dots, y$) in value for each pixel position (i, j).

Integration of Markov-CA and landform-based models

In this study, an approach was developed for improving the reliability of simulation and prediction of LULC. The integration of Markov-CA and landform-based models were applied to provide improved reliability of prediction (Figure 3). There were four stages in running the integration process: (a) making transition probability maps based on a landform-based model (in this case TPI), which were then used to manage the spatial differences in LULC; (b) making a transition potential map, which was then used to manage the spatial distribution of LULC; (c) making a transition area matrix, obtained from LULC data maps for the years *t* - *i* and *t* in the Markov model structure; (d) integrating the results of the un-transition probability map, transition potential map and transition area matrix was then the key step in generating the local transition rule for the CA model used to produce simulations and predictions of LULC. The LULC data maps for the years *t* - *i* and *t* were used as inputs to determine the transition area matrix and transition probability matrix used in the Markov model structure. The un-transition probability matrix for years *t* - *i* and *t* can be calculated from the results of the transition probability matrix for *t* - *i* and *t*.

Table 4. Definitions of landform classes in the TPI landform-based model (modified from Guisan et al. (1999), Weiss (2000), Wilson and Gallant (2000), Tagil and Jenness (2008), and De Reu et al. (2013)

Classes	**Descriptions**	**The probability of a landform class that influences changes in LULC**
Streams	Small neighbourhood TPI: TPI ≤ -1 Large neighbourhood TPI: TPI ≤ -1	0.11
Midslope drainages	Small neighbourhood TPI: TPI ≤ -1 Large neighbourhood TPI: -1 < TPI < 1	0.13
Upland drainages	Small neighbourhood TPI: TPI ≤ -1 Large neighbourhood TPI: TPI ≥ 1	0.15
Valleys	Small neighbourhood TPI: -1 < TPI < 1 Large neighbourhood TPI: TPI ≤ -1	0.16
Plains	Small neighbourhood TPI: -1 < TPI < 1 Large neighbourhood TPI: -1 < TPI < 1, slope ≤ 5º	0.18
Open slopes	Small neighbourhood TPI: -1 < TPI < 1 Large neighbourhood TPI: -1 < TPI < 1, slope > 5º	0.09
Upper slopes	Small neighbourhood TPI: -1 < TPI < 1 Large neighbourhood TPI: TPI ≥ 1	0.07
Local ridges	Small neighbourhood TPI: TPI ≥ 1 Large neighbourhood TPI: TPI ≤ -1	0.05
Midslope ridges	Small neighbourhood TPI: TPI ≥ 1 Large neighbourhood TPI: -1 < TPI ≥ 1	0.04
High ridges	Small neighbourhood TPI: TPI ≥ 1 Large neighbourhood TPI: TPI ≥ 1	0.02

Relationships between the TPI, which is a landform-based model, and the un-transition probability matrix are used to generate an un-transition probability map. These relationships were calculated based on the Pearson correlation. There was a linear correlation between TPI and un-transition probability matrix. The combination of TPI and matrix non-transition probability was done by a neural network algorithm to create an un-transition probability map. The un-transition probability map and the transition potential maps were then combined by multiplying them together. The results of this combination could then be entered together with the transition area matrix to simulate and predict LULC in the CA model structure.

Comparison of the three maps at multiple resolutions

In this study, comparison of the three maps at multiple resolutions was used to evaluate the accuracy and reliability of the integration experiment between the Markov-CA and landform-based models, performed to simulate and predict the LULC map. The three-map comparison method, as proposed by Pontius et al. (2008; 2011; 2018), requires (a) a reference map for the initial time (T1) at the start of the simulation for the calibration of the LULC change model; (b) a reference map of a subsequent time (T2) at the end time of the simulation for the validation model; and (c) a simulation map of the same T2 (S2) at the end time of the simulation produced by the LULC change model. Analysis of the three-map comparisons showed how changes in the simulation maps compared with changes in the reference maps, which were calculated based on the figure of merit (FOM). FOM is the most appropriate approach for validating the LULC change model and is better than metrics such as producer's accuracy, user's accuracy and Kappa that are very commonly applied in GIS and can be misleading in assessing the accuracy of LULC change models. FOM has five components: (a) persistence simulated correctly (correct rejections); (b) persistence simulated as change (false alarms); (c) change simulated as change to wrong category (wrong hits); (d) change simulated correctly (hits); and (e) change simulated as persistence (misses) (Pontius et al., 2008; Pontius and Millones, 2011; 2011; 2018).

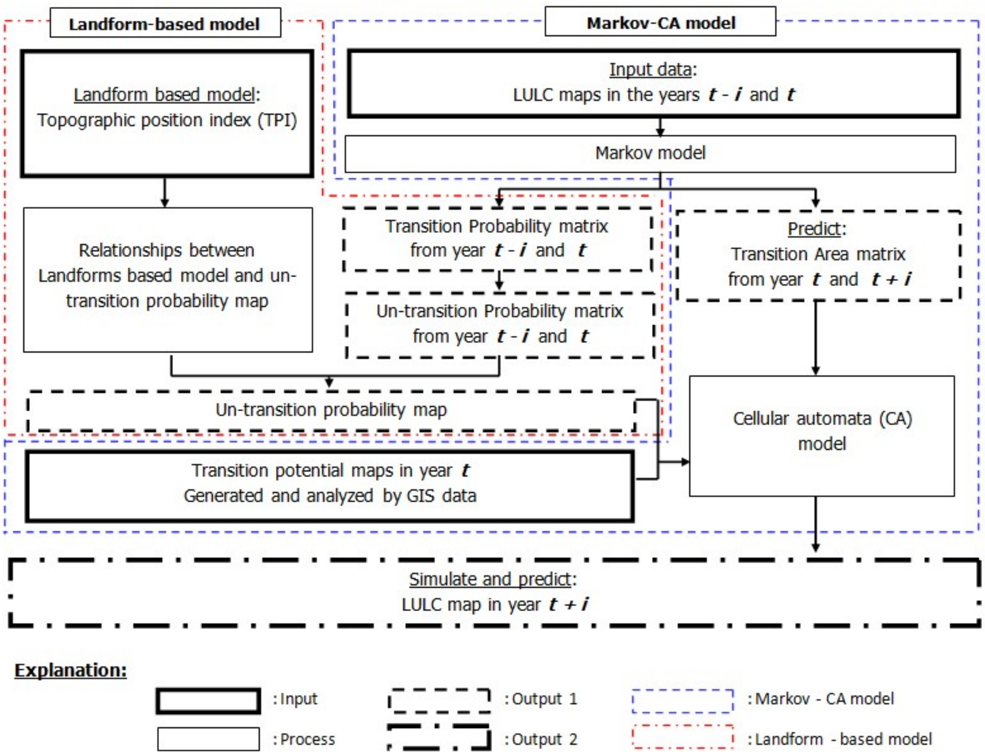

Figure 3. Flowchart of the integration experiment between the Markov-CA and landform-based models performed to simulate and predict the LULC map in this study

Results

Based on the data availability for LULC in 1996, 2000 and 2003 (Figure 2) taken from the study conducted by Yulianto et al. (2018), six data-pair combinations were used as inputs to simulate and predict LULC in 2009 and 2017: (a) LULC in 1996 and 2000 for LULC in 2009; (b) LULC in 1996 and 2003 for LULC in 2009; (c) LULC in 2000 and 2003 for LULC in 2009; (d) LULC in 1996 and 2000 for LULC in 2017; (e) LULC in 1996 and 2003 for LULC in 2017; and (f) LULC in 2000 and 2003 for LULC in 2017. Prediction of the transition area matrix produced by the Markov model can provide information about the probability of changes from one LULC class to another. The predictions for the transition area matrix and the transition probability matrix indicate that the matrix diagonally represents the transition probability in LULC with the same class. Meanwhile, the non-diagonal matrix describes the transition probability in a LULC class that has the potential to change to another class.

In this study, a landform-based model was used as the input to create the un-transition probability map. TPI is the landform-based model approach used in this study, as proposed by Guisan et al. (1999), Weiss (2000), and Wilson and Gallant (2000). Landform classification and interpretation were calculated from TPI grids using four different neighbourhoods (100 m, 300 m, 500 m and 700 m). The size and shape of neighbourhoods are very important for analysis based on the scale of the features of the landforms analyzed. Small neighbourhoods (100 m) were used to classify small landforms features and to extract the edges of features rather than the features themselves. In contrast, large neighbourhoods (700 m) were used to identify landforms and extract terrace and depression features such as valleys or hills. The combination of TPI at the scale of small and large neighbourhoods is required in order to distinguish the classified landforms. The results of the classification of landforms yielded ten classes: streams, midslope drainages, upland drainages, valleys, plains, open slopes, upper slopes, local ridges, midslope ridges and high ridges. The results of the landform-based model classifications using TPI in various neighbourhood scenarios can be found in Figure 4. Meanwhile, the probability value of the landform model based on the combination of TPI on the scale of small and large neighbourhoods to distinguish the classified landforms can be found in Figure 5. The factors or parameters used in this study to create the potential transition map were elevations, slope, distance from the nearest roads, distance from water bodies and distance from urban areas. The results of GIS analysis based on MCE, AHP and fuzzy membership functions can be found in Table 3 and Figure 6. The results of the simulation and prediction of LULC generated based on the Markov-CA model without the integration of the landform-based model can be found in Figures 7A, 7B and 7C for 2009 (with a combination of input data pairs for 1996, 2000 and 2003) and Figures 8A, 8B and 8C for 2017 (with a combination of input data pairs for 1996, 2000 and 2003). Meanwhile, the results of the simulation and prediction of LULC generated based on the integration of the Markov-CA and landform-based models can be found in Figures 7D, 7E and 7F for 2009 (with a combination of input data pairs for 1996, 2000 and 2003) and Figures 8D, 8E and 8F for 2017 (with a combination of input data pairs for 1996, 2000 and 2003). The results of the comparison of the three-map calculations at multiple resolutions presented in Figures 9, 10 and 11, show how the changes in the simulation maps compared with the changes in the reference map. 18 pairs of data were used for the comparison of the three maps at multiple resolutions: (a) a reference map of the initial time (T1); (b) a reference map of a subsequent time (T2); and (c) a simulation map of the same time as T2 (S2).

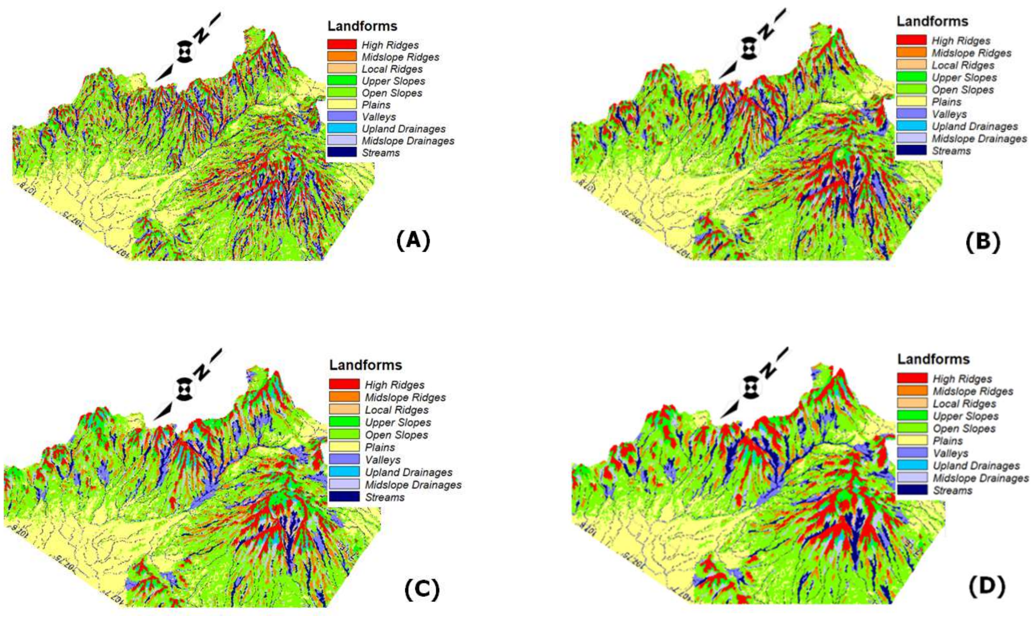

Figure 4. Landform-based model classifications using TPI in various neighbourhood scenarios: A) TPI values for neighbourhoods at the scale of 100 m; B) TPI values for neighbourhoods at the scale of 300 m; C) TPI values for neighbourhoods at the scale of 500 m; D) TPI values for neighbourhoods at the scale of 700 m

Furthermore, analysis of the calculation of FOM was performed to provide information on components related to correct rejections, false alarms, wrong hits, hits and misses. For example, the three maps consisting of T1: 1996; T2: 2009; and S2: 2009 (1996 and 2000) provided the reference map of the initial time. (T1) is LULC in 1996, the reference map of T2 is LULC in 2009, and the simulation map of T2 (S2) is simulated LULC in 2009 with the input data for LULC in 1996 and 2000.

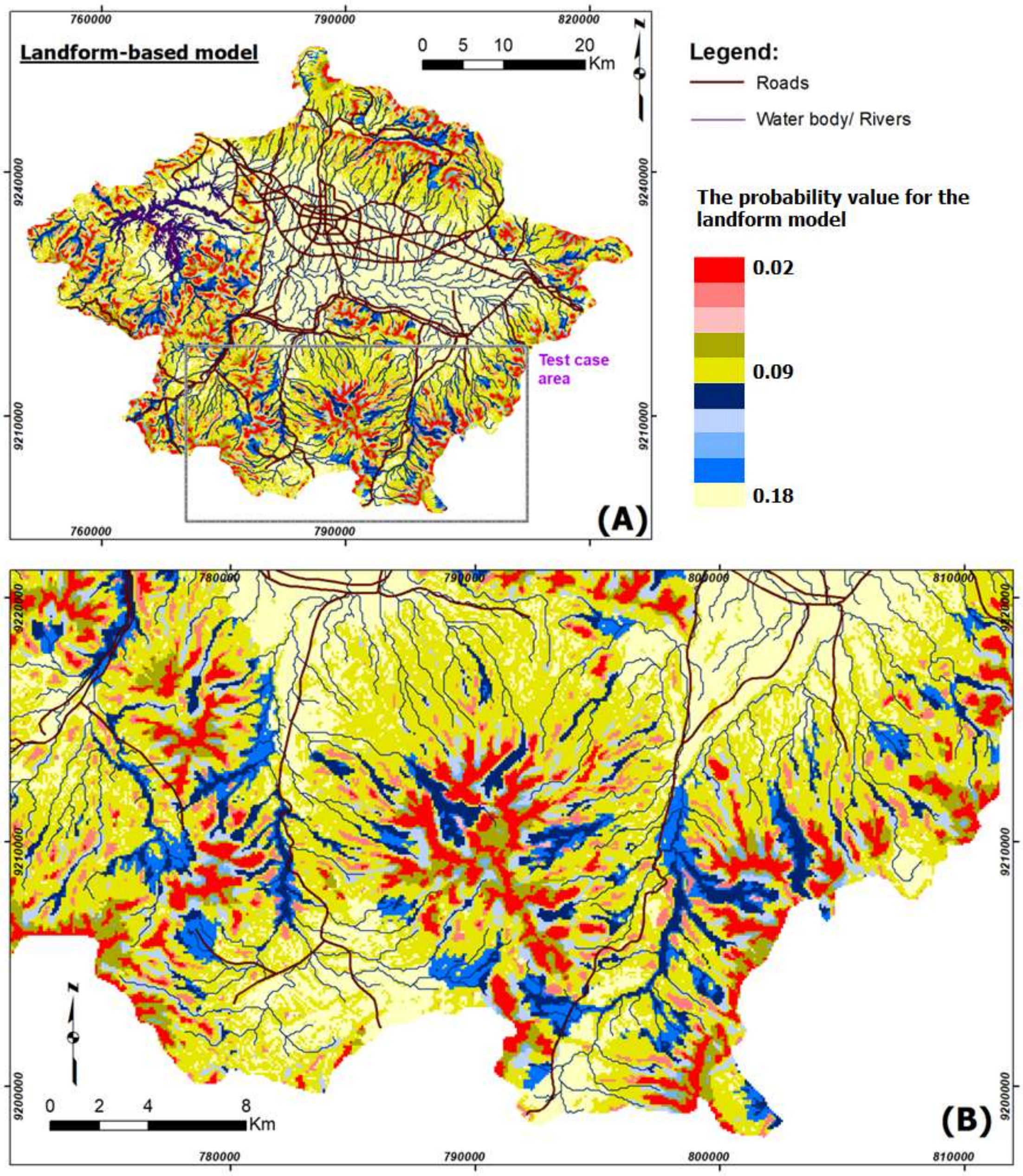

Figure 5. The probability values for the landform model based on the combination of TPI at the scale of small and large neighbourhoods, used to distinguish the classified landforms: A) Landform-based model classifications from the combination at the scale of small and large neighbourhoods; B) Display zoom view map of the Landform-based model for the test case area

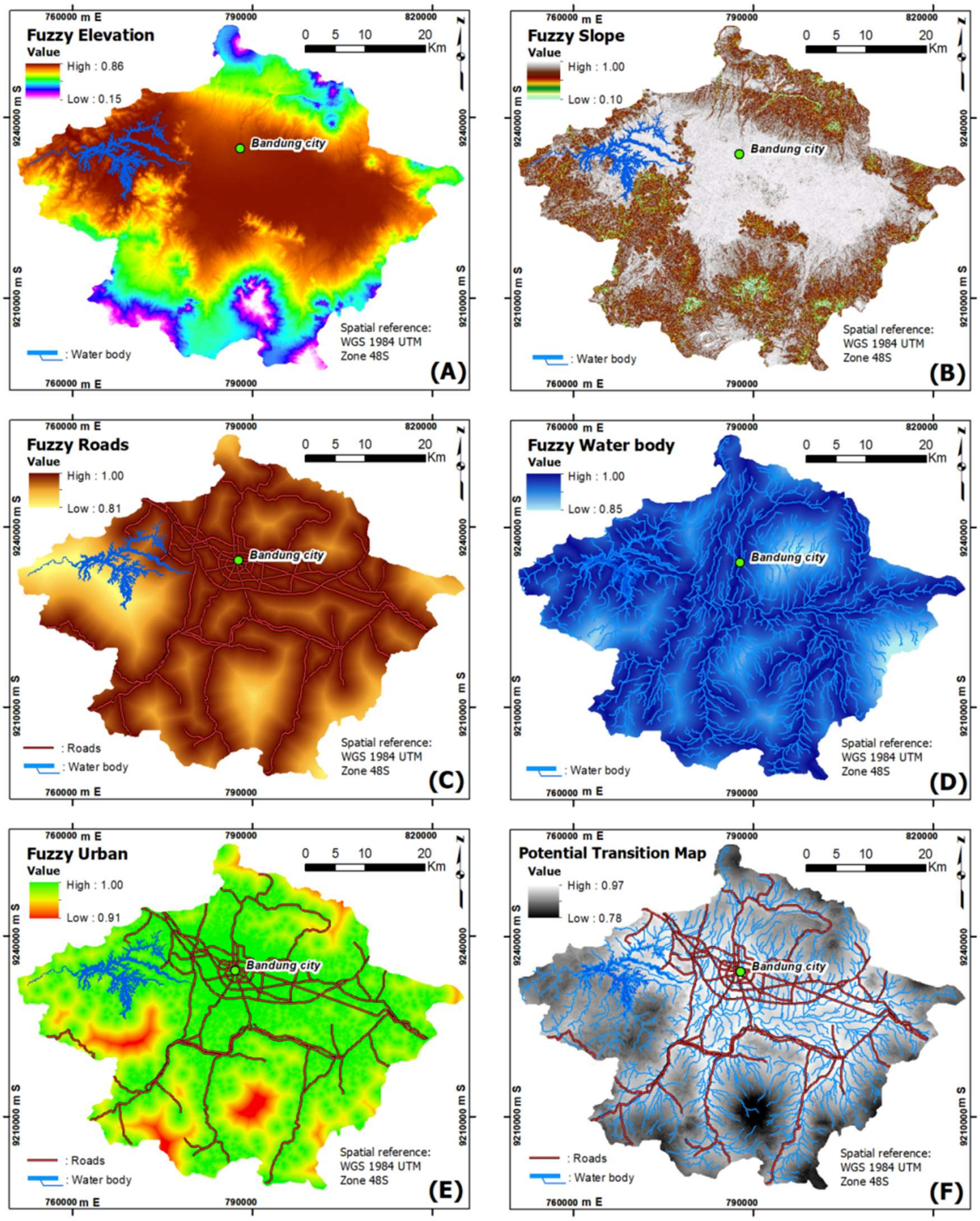

Figure 6. The factors or parameters used to create the potential transition map: A) elevation; B) slope; C) distance from the nearest roads; D) distance from water bodies; E) distance from urban areas; F) potential transition map

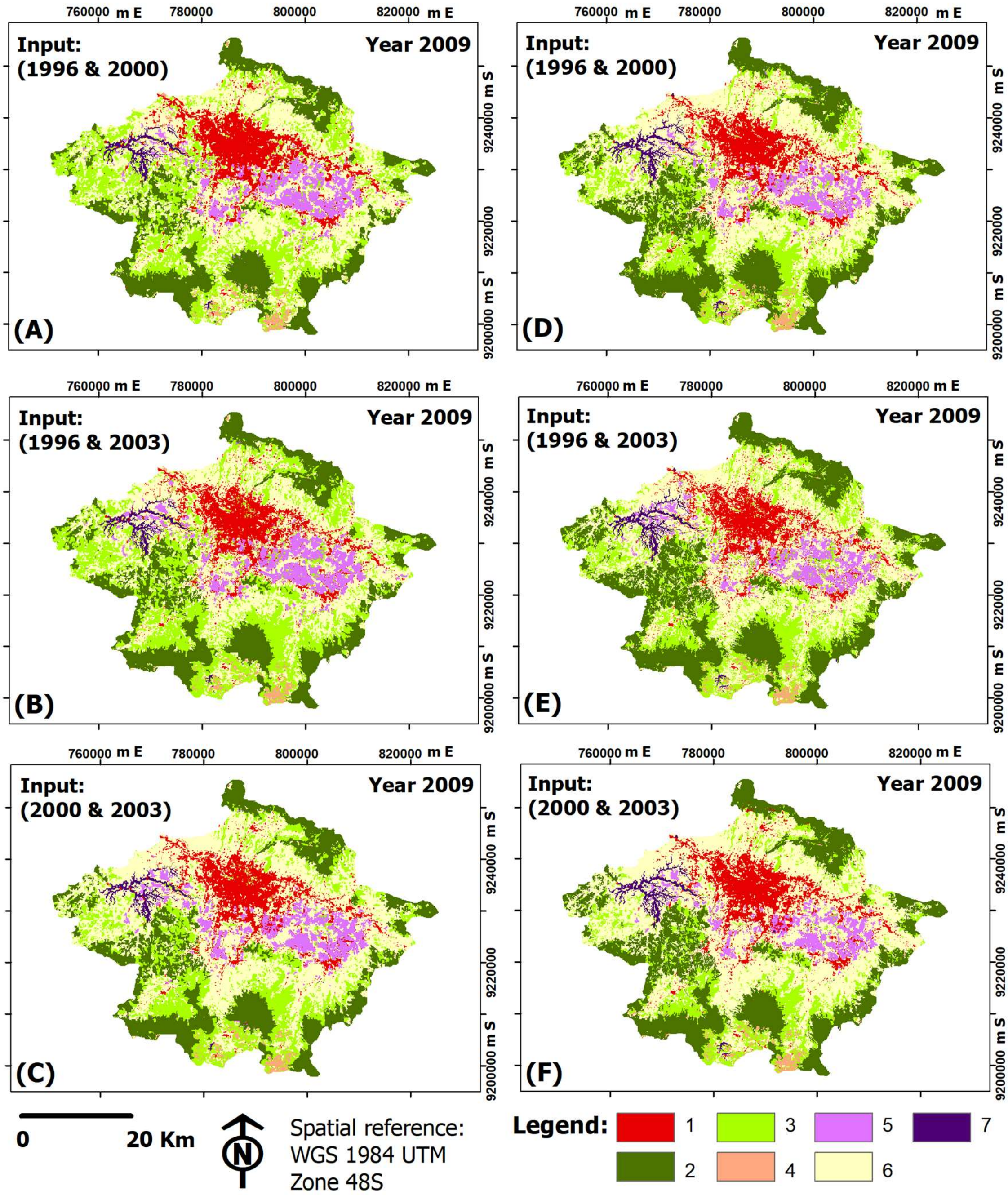

Figure 7. The results of simulating and predicting LULC in 2009 based on the combination input data pairs for 1996, 2000 and 2003: A), B) and C): LULC in 2009 from the Markov-CA model without integration of the landform-based model; D), E) and F): LULC in 2009 from the integration of the Markov- CA and landform-based models. Class 1: built land; class 2: primary forest; class 3: secondary forest and mixed garden; class 4: plantation; class 5: wet agricultural land; class 6: dryland farming; class 7: water body

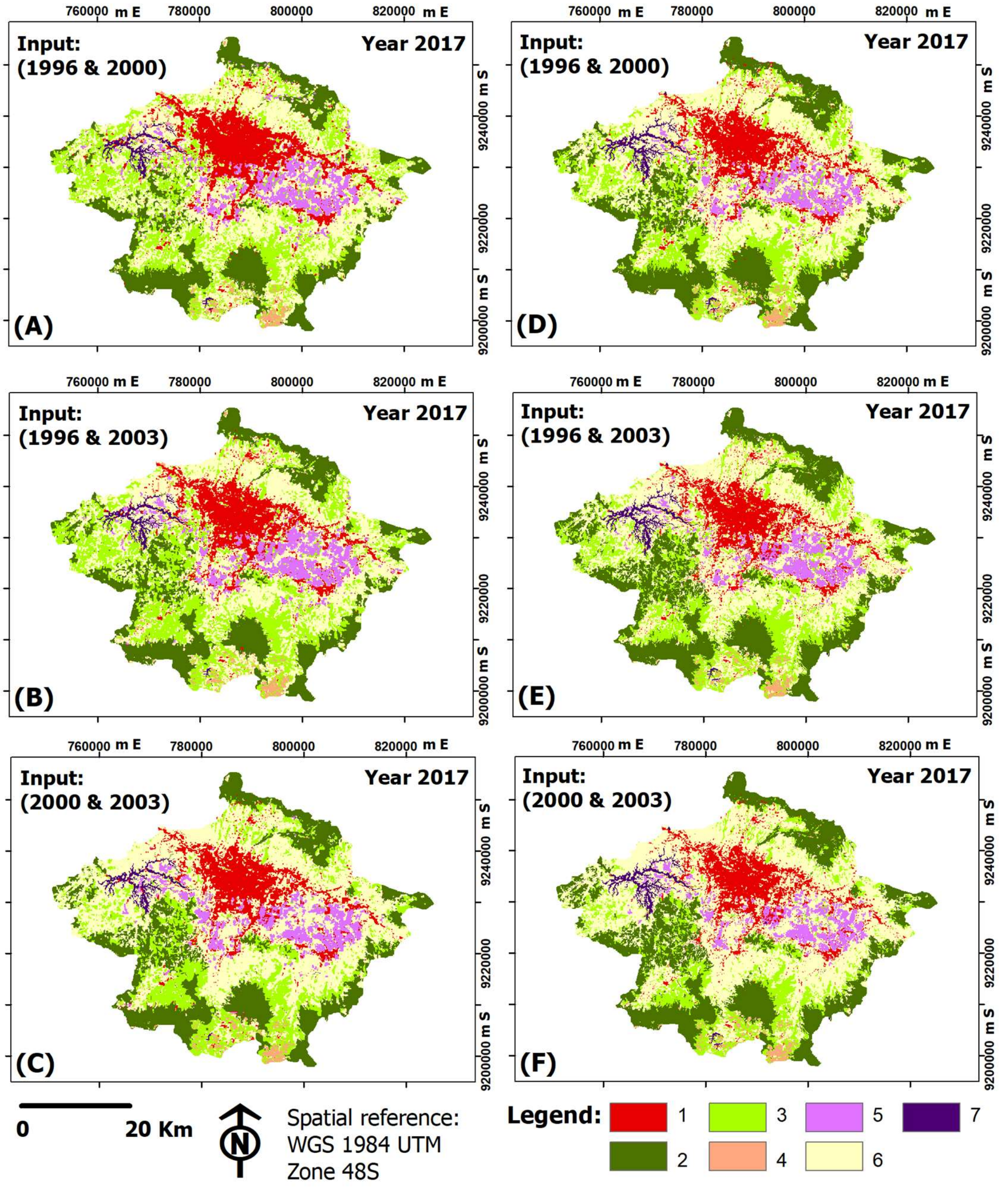

Figure 8. The results of simulating and predicting LULC in 2017 based on the combination input data pairs for 1996, 2000 and 2003: A), B) and C) LULC in 2017 from the Markov-CA model without integration of the landform-based model; D), E) and F) LULC in 2017 from the integration of the Markov-CA and landform-based models. Class 1: built land; class 2: primary forest; class 3: secondary forest and mixed garden; class 4: plantation; class 5: wet agricultural land; class 6: dryland farming; class 7: water body

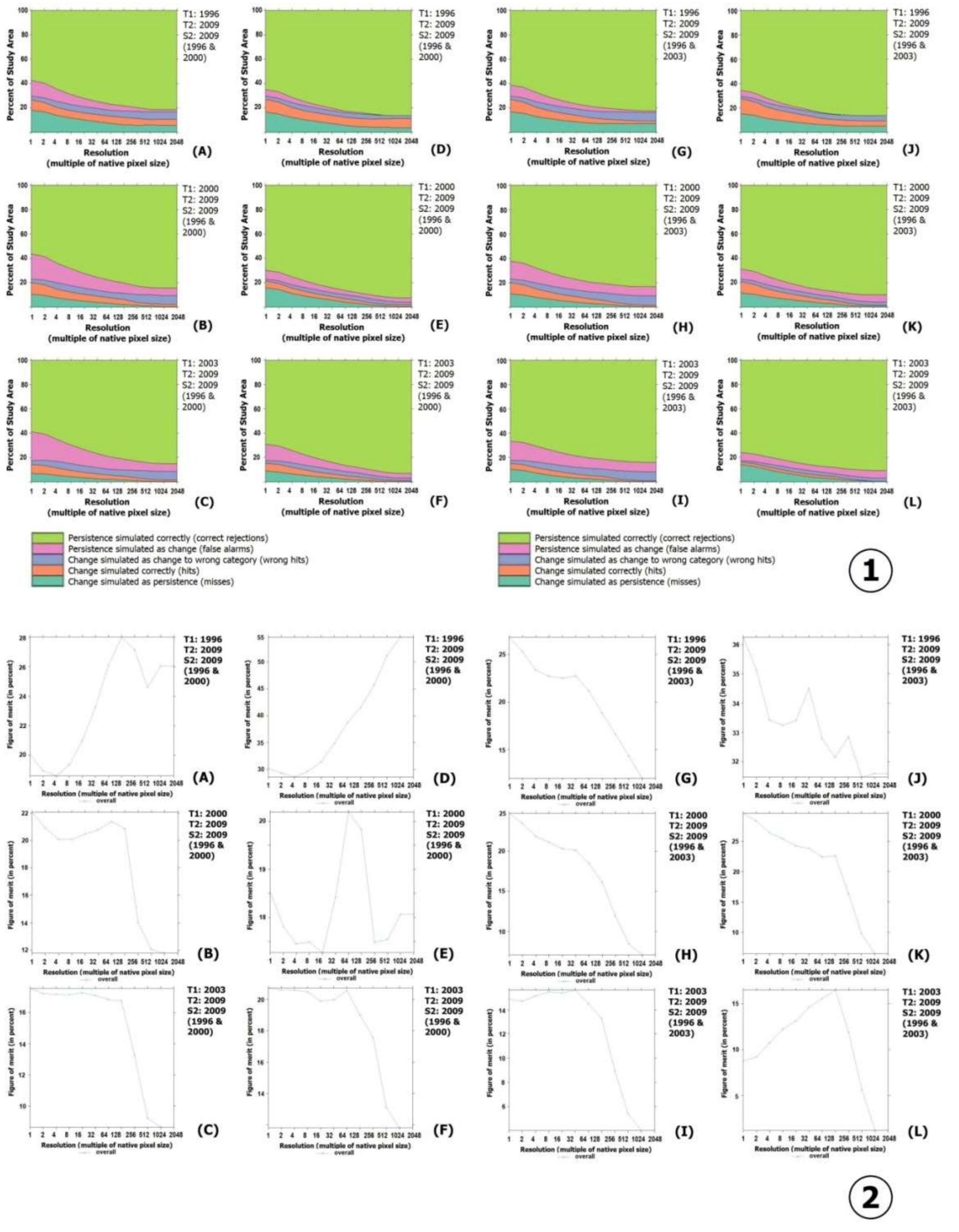

Figure 9. The results of the comparison of the three-map calculations at multiple resolutions. 1) shows the relationship of the percentage of the study area, resolution (multiple of native pixel size) and components related to correct rejections, false alarms, wrong hits, hits and misses, while 2) shows the relationship of the FOM and resolution (multiple of native pixel size). A), B) and C) and G), H) and I) are the results of the comparison of the three-map calculations and FOM without the integration of the Markov-CA and landform-based models, while D), E) and F) and J), K) and L) are the results of the comparison of the three-map calculations and FOM with the integrated Markov-CA and landform-based models. Resolution is one multiple of native pixel size equivalent to 30 m pixel size

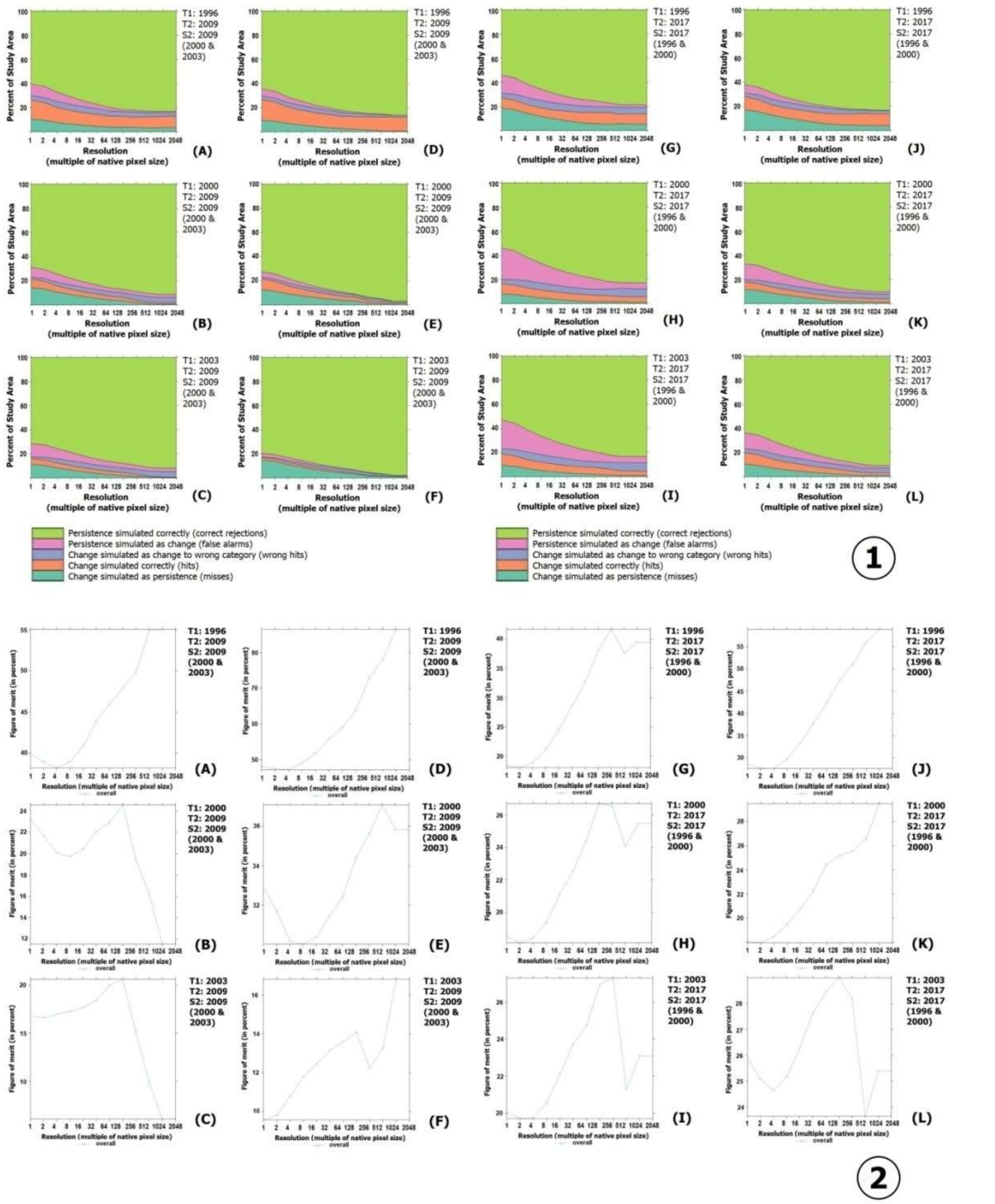

Figure 10. The results of the comparison of the three-map calculations at multiple resolutions. 1) shows the relationship of the percentage of the study area, resolution (multiple of native pixel size) and components related to correct rejections, false alarms, wrong hits, hits and misses, while 2) shows the relationship of the FOM and resolution (multiple of native pixel size). A), B) and C) and G), H) and I) are the results of the comparison of three maps calculation and FOM without the integration from Markov-CA and landform-based model, while D), E) and F) and J), K) and L) are the results of the comparison of the three-map calculations and FOM with the integrated Markov-CA and landform-based models. The resolution is one multiple of native pixel size equivalent to 30 m pixel size

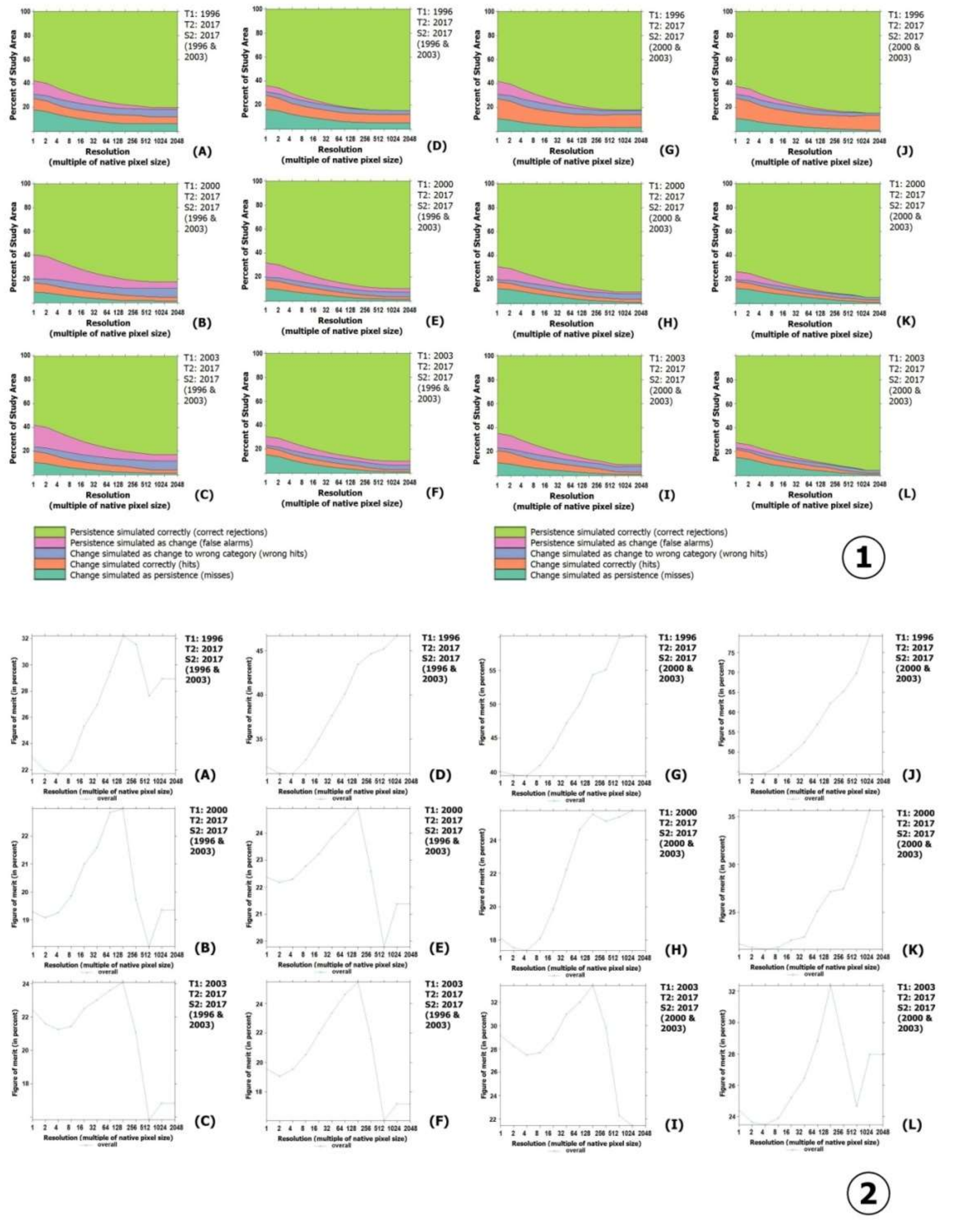

Figure 11. The results of the comparison of the three-map calculations at multiple resolutions. 1) shows the relationship of the percentage of the study area, resolution (multiple of native pixel size) and components related to correct rejections, false alarms, wrong hits, hits and misses, while 2) shows the relationship of the FOM and resolution (multiple of native pixel size). A), B) and C) and G), H) and I) are the results of the comparison of the three-map calculations and FOM without integration form of the Markov-CA and landform-based models, while D), E) and F) and J), K) and L) are the results of the comparison of the three-map calculations and FOM with the integrated Markov-CA and landform-based models. The resolution is one multiple of native pixel size equivalent to 30 m pixel size

Discussion

Performance in improving the accuracy and reliability of LULC simulations

The phenomenon of LULC change in the upper Citarum watershed has received serious attention from the government of Indonesia and is one of the country's watersheds that has received attention and priority at a national scale. Previous research into LULC changes in the study area has been carried out by Yulianto et al. (2018). The results of this present research indicate related LULC changes that describe past and present conditions and provide predictions for the future. The effort to improve the accuracy and reliability of simulated LULC is the main objective of this research. The results of this study can be used to improve the accuracy and reliability of the simulated LULC model to support several previous studies. Thus, the approach integrating the Markov-CA and landform-based models is demonstrated in this study to achieve the research objectives.

There are two components of agreement and three components of disagreement based on the three-map comparison approach. Correct rejections and hits are the components that indicate agreement, while misses, wrong hits and false alarms indicate disagreement. Meanwhile, misses, hits and wrong hits are the components which indicate observed change, while hits, wrong hits and false alarms indicate simulated change (Pontius and Millones, 2011; Pontius et al., 2008; 2011; 2018).

Pairs of LULC data for 1996, 2000 and 2003 derived from remote sensing data used in the study conducted by Yulianto et al. (2018) were input to simulate and predict LULC in 2009 and 2017. Meanwhile, LULC in 2009 and 2017 was used as the reference base for evaluating the accuracy and reliability of the LULC model developed in this study. Performance measurement in terms of improved LULC simulation accuracy and reliability can be carried out using the three-map calculation comparison approach at multiple resolutions, as presented in Figures 9, 10 and 11. Meanwhile, Figure 12 and Table 5 show the comparison and differences between the example of interpretation results from the calculations of the three-map comparison approach for the 30 m pixel size resolution before and after the Markov-CA and landform-based models were integrated.

In general, the information presented in Figures 9, 10 and 11 indicates that integration of the Markov-CA and landform-based models increased correct rejection as a component of agreement and reduced wrong hits and false alarms as components of disagreement for the percentage of the study area at each resolution (multiple of native pixel size). Hits as a component of agreement change simulated correctly also show an increase, even though nine of the 18 pairs of three-map comparisons show a decline. Meanwhile, misses as a component of disagreement simulated as persistence also show an increase, although six of the 18 pairs of data show a decline. Meanwhile, based on the overall three-map comparison analysis, it can be shown that there is an increase in FOM values after the Markov-CA and landform-based models were integrated, although six of the 18 pairs of data indicate a decrease in FOM values.

The interpretation of ID A-1 (T1: 1996; T2: 2009; S2: 2009 (1996 and 2000)) (Figure 12 and Table 5), indicates that Markov-CA and landform-based model integration increased the agreement components (correct rejections and hits), at 7.4% and 2%, respectively. Meanwhile, it also reduced disagreement components (misses, wrong hits and false alarms), at 1.6%, 0.5% and 7.3%, respectively; thus, the increase in FOM is 10.1%. It can be shown that the results of calculations on the 18 pairs of three-map comparisons have an increased value of FOM for 12 pairs of data after the Markov-CA and landform-based models were integrated, while six data pairs had decreased FOM values. The integration of the Markov-CA and landform-based models in several combinations and data pairs increased the FOM values for LULC simulations for 2009 from 3.1% to 10.1% and for LULC simulations for 2017 from 3.1% to 10.3%.

Limitations and potential application

In this study, LULC simulation was performed using the Markov-CA approach integrated with a landform-based model. Improvement of the accuracy and reliability of simulated LULC can be shown to have been achieved from the comparison of models before and after integration between the Markov-CA and landform-based models. Other potential applications in several LULC modelling technical approaches can be investigated in future research using not only Markov-CA, but also others approaches, such as the spatial logistic regression model (Tayyebi et al., 2010), the econometric-based land-use model (Plantinga and Lewis, 2014), the dynamic simulation model (Stéphenne and Lambin, 2001), linear programming and GIS (Chuvieco, 1993) and others. The landform-based model applied is limited in this study to the TPI model as proposed by Guisan et al. (1999), Weiss (2000), Wilson and Gallant (2000). Thus, the integration of other landform-based models, such as terrain surface classification as proposed by Iwahashi and Pike (2007), could be applied in future research. The spatial resolution of the data used in this study is

30 m based on input (Landsat and SRTM30 DEM imagery) which can produce information at a map scale of 1:25,000 to 1:50,000. To produce more detailed information for map scales of 1:5,000 to 1:10,000, future research should use high-resolution image data such as SPOT 6/7 images, Pleiades, Worldview and others. In addition, the DEM data for obtaining detailed topographic information could be derived based on stereo data from SPOT 6/7 images, as carried out by Yulianto et al. (2016). Integration of the Markov-CA and landform-based models for LULC simulations was applied to a small (local) area in this study; thus, it is necessary to test this model for a wider location to determine the performance of the model approach proposed in this study.

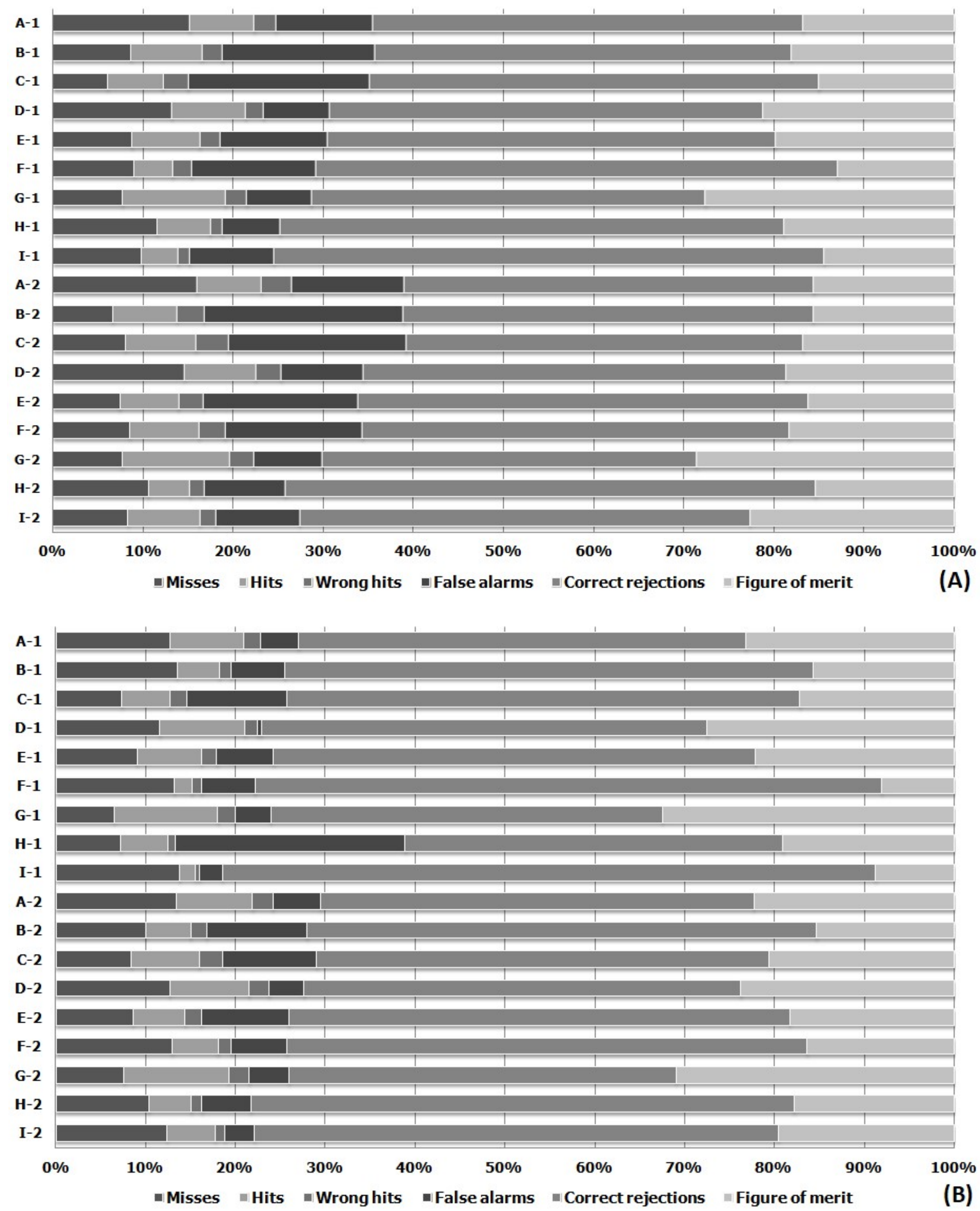

Figure 12. Example of interpretation results from the calculation of the three-map comparison approach at multiple resolutions (for the 30 m pixel size resolution) showing the relationship of the percentage of the study area for the 30 m pixel size resolution and components related to correct rejections, false alarms, wrong hits, hits, misses and FOM. There are 18 pairs of data used for the comparison of the three maps, for T1, T2 and S2. A) Results of the comparison of the three-map calculations and FOM without integration of the Markov-CA and landform-based models. B) Results of the comparison of the three-map calculations and FOM with integrated Markov-CA and landform-based models

Table 5. The results of comparison and difference values of the component FOM (misses, hits, wrong hits, false alarms and correct rejections) for the 18 pairs of data used for LULC simulation and prediction for 2009 and 2017, before and after the Markov-CA and landform-based models were integrated (for 30 m pixel size resolution)

ID	Three-map comparison	Comparison Values (%)					
		Misses	Hits	Wrong hits	False alarms	Correct rejections	FOM
A-1	T1: 1996. T2: 2009. S2: 2009 (1996 & 2000)	-1.60	2.00	-0.50	-7.30	7.40	10.10
B-1	T1: 2000. T2: 2009. S2: 2009 (1996 & 2000)	5.50	-4.00	-1.30	-13.50	13.50	-3.40
C-1	T1: 2003. T2: 2009. S2: 2009 (1996 & 2000)	1.80	-0.80	-1.00	-10.30	10.20	3.10
D-1	T1: 1996. T2: 2009. S2: 2009 (1996 & 2003)	-1.40	2.10	-0.60	-8.80	4.50	9.50
E-1	T1: 2000. T2: 2009. S2: 2009 (1996 & 2003)	0.70	-0.20	-0.60	-6.70	6.70	3.70
F-1	T1: 2003. T2: 2009. S2: 2009 (1996 & 2003)	4.00	-2.80	-1.20	-9.40	9.10	-6.10
G-1	T1: 1996. T2: 2009. S2: 2009 (2000 & 2003)	-1.00	1.30	-0.50	-4.00	4.00	10.00
H-1	T1: 2000. T2: 2009. S2: 2009 (2000 & 2003)	-1.70	1.70	-0.20	36.20	3.50	9.60
I-1	T1: 2003. T2: 2009. S2: 2009 (2000 & 2003)	3.70	-2.90	-1.00	-8.10	8.20	-7.20
A-2	T1: 1996. T2: 2017. S2: 2017 (1996 & 2000)	-1.60	2.40	-1.00	-8.10	8.20	10.30
B-2	T1: 2000. T2: 2017. S2: 2017 (1996 & 2000)	4.00	-2.60	-1.40	-13.10	13.00	-0.40
C-2	T1: 2003. T2: 2017. S2: 2017 (1996 & 2000)	1.00	0.10	-1.00	-10.50	10.60	5.80
D-2	T1: 1996. T2: 2017. S2: 2017 (1996 & 2003)	-1.30	1.90	-0.60	-6.10	6.00	8.20
E-2	T1: 2000. T2: 2017. S2: 2017 (1996 & 2003)	1.70	-0.70	-1.10	-8.60	8.60	3.10
F-2	T1: 2003. T2: 2017. S2: 2017 (1996 & 2003)	5.10	-3.30	-1.70	-11.30	11.40	-2.80
G-2	T1: 1996. T2: 2017. S2: 2017 (2000 & 2003)	0.30	0.10	-0.40	-4.20	4.10	4.70
H-2	T1: 2000. T2: 2017. S2: 2017 (2000 & 2003)	0.20	0.20	-0.30	-4.10	4.10	3.60
I-2	T1: 2003. T2: 2017. S2: 2017 (2000 & 2003)	4.70	-3.60	-1.00	-7.90	7.90	-4.80

(+) = increased value; (-) = decreased value. Correct rejection and hits are the two components indicating an agreement. Misses, wrong hits and false alarms are the three components indicating a disagreement. Misses, hits and wrong hits are the three components indicating observed change. Hits, wrong hits and false alarms are the three components indicating simulated change

Conclusion

This paper has presented the results of a new approach for LULC simulations applied in the upper Citarum watershed, West Java Province, Indonesia. The integration of Markov-CA and landform-based models has been used to simulate LULC in the study area. In this model, the un-transition probability map is based on the correlation between the landform-based model and the un-transition probability matrix used to simulate LULC. The model has been successfully applied by comparing LULC simulation results for the Markov-CA approach before and after being integrated with the landform-based model. The results of the comparison of three-map calculations at multiple resolutions have shown that results are better after the integration of Markov-CA and landform-based models than before integration. This confirms an increase in the accuracy and reliability of the LULC simulation model produced. The limitations of this study are that the integration of the model as currently applied covers an area that is not wide, so the development of further research by applying this model to a wider research area can be considered.

Acknowledgements

This paper is a part of the research activities entitled 'The utilization of remote sensing data for disaster mitigation in Indonesia'. This research was funded by the Program of National Innovation System Research Incentive (INSINAS) in 2018, Ministry of Research, Technology, and Higher Education, Republic of Indonesia contract No. 11 / INS-1 / PPK / E4 / 2018 dated March 9, 2018.. Thanks go to Dr M. Rokhis Khomarudin as director of the Remote Sensing Application Center LAPAN, Dr Dony Kushardono as the group leader for this activity, and colleagues at the Remote Sensing Application Center, LAPAN, for discussions and suggestions. SRTM30 DEM was provided by the US Geological Survey (USGS). Landsat 8 OLI/TIRS was provided by Remote Sensing Technology and Data Center, LAPAN. Thanks also to the Statistics Service Unit, Ministry of Communication and Information, West Java Province, Indonesia, for discussion, collaboration, field surveys and sharing of spatial data to support this research.

References

Abubakr, A.A.A. and Biswajeet, P. 2015. A novel Approach for Predicting the Spatial Patterns of Urban Expansion by Combining the Chi-Squared Automatic Integration Detection Decision Tree, Markov Chain, and Cellular Automata Models in GIS. *Geocarto International* 30(8), DOI: 10.1080/10106049.2014.997308.

Ademiluyi, I.A. and Otun, W.O. 2009. Spatial decision support systems (SDSS) and sustainable development of the third world. *Journal of Sustaintainable Development in Africa* 10(4):200–217.

Arsanjani, J.J., Helbich, M., Kainz, W. and Boloorani, A.D. 2013. Integration of logistic regression, Markov chain and cellular automata models to simulate urban expansion. *International Journal of Applied Earth Observation and Geoinformation* 21: 265–275.

Behera, M.D., Borate, S.N., Panda, S.N., Behera, P.R. and Roy, P.S. 2012. Modelling and analyzing the watershed dynamics using Cellular Automata (CA)-Markov model - a geo-information based approach. *Journal of Earth System Science* 121: 1011–1024.

Blaszczynski, J.S. 1997. Landform characterization with geographic information systems. *Photogrammetric Engineering & Remote Sensing* 63(2): 183-191.

Brabyn, L. 1998. GIS Analyses of Macro Landform. Presented at SIRC 98 – The 10th Annual Colloquium of the Spatial Information Research Centre, University of Otago, Dunedin, New Zealand.

Burrough, P.A., van Gaans, P.F.M. and; MacMillan, R.A. 2000. High-resolution landform classification using fuzzy k-means. *Fuzzy Sets and Systems* 113: 37–52.

Chapin, F.S., Zavaleta, E.S., Eviner, V.T., Naylor, R.L., Vitousek, P.M., Reynolds, H.L., Hooper, D.U., Lavorel, S., Sala, O.E., Hobbie, S.E., Mack, M.C. and Diaz, S. 2000. Consequences of changing biodiversity *Nature* 405: 234-242.

Chorley, R.J. 1972. Chapter 1-Spatial Analysis in Geomorphology. In: Chorley, R.J. (ed.). *Spatial Analysis in Geomorphology*. Harper and Row Publishers, New York, USA, pp: 3-16.

Chuvieco, E. 1993. Integration of linear programming and GIS for land-use modeling. *International Journal of Geographical Information Systems* 7(1):71-83.

Coates, D.R. 1958. Quantitative geomorphology of small drainage basins in Southern Indiana. 1st Ed., Columbia University, New York.

De Reu, J., Bourgeois, J., Bats, M., Zwertvaegher, A., Gelorini, V., De Smedt, P., Chu, W., Antrop, M., De Maeyer, P., Finke, P., Van Meirvenne, M., Verniers, J. and Crombé, P. 2013. Application of the topographic position index to heterogeneous landscapes. *Geomorphology* 186: 39-49. https://doi.org/10.1016/j.geomorph.2012.12.015.

Drăguţ, L. and Eisank, C. 2012. Automated object-based classification of topography from SRTM data. *Geomorphology* 141-142: 21–33.

Ehsani, A.H. and Quiel, F. 2008. Geomorphometric feature analysis using morphometric parameterization and artificial neural networks. *Geomorphology* 99: 1–12.

Evans, I.S. 1972. Chapter 2-General Geomorphometry, Derivatives of Altitude and Descriptive Statistics. In: Chorley, R.J. (ed.), *Spatial Analysis in Geomorphology*. Harper and Row, Publishers, New York, USA, pp: 17-90.

Foley, J.A., DeFries, R., Asner, G.P., Barford, C., Bonan, G., Carpenter, S.R., Chapin, F.S., Coe, M.T., Daily, G.C., Gibbs, H.K., Helkowski, J.H., Holloway, T., Howard, E.A., Kucharik, C.J., Monfreda, C., Patz, J.A., Prentice, I.C., Ramankutty, N. and Snyder, P.K. 2005. Global consequences of land use. *Science* 309: 570–574.

Foody, G.M. 2002. Status of land cover classification accuracy assessment. *Remote Sensing of Environment* 80:185 – 201.

Gemitzi, A., Falalakis, G., Eskioglou, P. and Petalas, C. 2011. Evaluating landslide susceptibility using environmental factors, fuzzy membership functions and GIS. *Global Nest Journal* 12: 1-13.

Giguere, P. and Dudek, G. 2009. Clustering sensor data for autonomous terrain identification using time-dependency. *Autonomous Robots* 26: 171–186.

Guisan, A., Weiss, S.B. and Weiss A.D. 1999. GLM versus CCA spatial modeling of plant species distribution. *Plant Ecology* 143: 107–122.

Horton, R.E. 1945. Erosional development of streams and their drainage basins: Hydrophysical approach to quantitative morphology. *Geological Society of America Bulletin* 56: 275–370.

Irvin, B.J., Ventura, S.J. and Slater, B.K. 1997. Fuzzy and isodata classification of landform elements from digital terrain data in Pleasant Valley, Wisconsin. *Geoderma* 77: 137–154

Iwahashi, J. and Pike, R.J. 2007. Automated classifications of topography from DEMs by an unsupervised nested-means algorithm and a three-part geometric signature. *Geomorphology* 86: 409–440.

Jasiewicz, J. and Stepinski, T.F. 2013. Geomorphons-a pattern recognition approach to classification and mapping of landforms. *Geomorphology* 182:147-156, 10.1016/j.geomorph.2012.11.005.

Jenness, J. 2010. Topographic Position Index (tpi_jen.avx) extension for ArcView 3.x", v. 1.3a. Jenness Enterprises, http://www.jennessent.com/arcview/tpi.htm.

Keshtkar, H. and Voigt W. 2016. A spatiotemporal analysis of landscape change using an integrated Markov chain and cellular automata models. *Modeling Earth System and Environment* 2: 10, doi: 10.1007/s40808-015-0068-4.

Li, D., Li, X., Liu, X.P., Chen, Y.M., Li, S.Y., Liu, K., Qiao, J.G., Zheng, Y.Z., Zhang, Y.H. and Lao, C.H. 2012. GPU-CA model for large-scale land-use change simulation. *Chinese Science Bulletin* 57*:* 2442–2452.

Li, X. and Yeh, A.G.O. 2002. Neural-network-based cellular automata for simulating multiple land-use changes using GIS. *International Journal of Geographical Information Science* 16: 323–343.

MacMillan, R.A. and Shary, P.A. 2009. *Landforms and Landform Elements in Geomorphometry*. Developments in Soil Science. Elsevier BV, 33. doi: 10.1016/S0166-2481(08)00009-3

MacMillan, R.A., Pettapiece, W.W., Nolan, S.C. and Goddard, T.W. 2000. A generic procedure for automatically segmenting landforms into landform elements using DEMs, heuristic rules and fuzzy logic. *Fuzzy Sets and Systems* 113: 81–109.

Memarian, H., Balasundram, S.K., Talib, J.B., Sung, C.T.B., Sood, A.M. and Abbaspour, K. 2012. Validation of CA-Markov for Simulation of Land Use and Cover Change in the Langat Basin, Malaysia. *Journal of Geographic Information System* 4: 542–554.

Mesgari, M.S., Pirmoradi, A. and Fallahi, G.R. 2008. Implementation of overlay function based on fuzzy logic in spatial decision support system. *World Applied Sciences Journal* 3(Supple 1): 60-65.

Miller, J.C. 1953. A quantitative geomorphic study of drainage basin characteristics in the cinch mountain area. Virginia and Tennessee, *Technical Report 3*.

Mokarram, M. and Sathyamoorthy, D. 2015. Relationship between landform classification and vegetation (case study: southwest of Fars province, Iran). *Open Geoscience* 8: 302–309.

Mousivand, A.J., Sarab, A.A. and Shayan S. 2007. A new approach of predicting land use and land cover changes by satellite imagery and Markov chain model (case study: Tehran). MSc Thesis. Tarbiat Modares University, Tehran, Iran.

Oinam, B.C., Marx, W., Scholten, T. and Wieprecht, S. 2014. A fuzzy rule base approach for developing a soil protection index map: a case study in the upper awash basin, Ethiopian highlands. *Land Degradation and Development* 25: 483–500.

Penner, J.E. 1994. Atmospheric chemistry and air quality. In: W. B. Meyer, B.L. Turner II (Eds.), *Changes in Land Use and Land Cover: A Global Perspective*. Cambridge: Cambridge University Press, pp. 175 – 209.

Plantinga, A.J. and Lewis, D.J. 2014. Landscape Simulations with Econometric-Based LandUse Models. Chapter 15 in the Oxford Handbook of Land Economics, Oxford University Press, New York.

Pontius, R.G. and Millones, M. 2011. Death to Kappa: birth of quantity disagreement and allocation disagreement for accuracy assessment. *International Journal of Remote Sensing* 32(15): 4407-4429. doi:10.1080/01431161.2011.552923.

Pontius, R.G., Boersma, W., Castella, J.C., Clarke, K., Nijs, T., Dietzel, C. and Verburg, P.H. 2008. Comparing the input, output, and validation maps for several models of land change. *The Annals of Regional Science* 42(1): 11–37. doi:10.1007/s00168-007-0138-2.

Pontius, R.G., Castella, J.C., de Nijs, T., Duan, Z., Fotsing, E., Goldstein, N., Kok, K. et al. 2018. Lessons and Challenges in Land Change Modeling Derived from Synthesis of Cross-Case Comparisons. In Trends in Spatial Analysis and Modelling, edited by Martin Behnisch and Gotthard Meinel 19:143–64. Geotechnologies and the Environment. Cham: Springer International Publishing, doi:10.1007/978-3-319-52522-8_8.

Pontius, R.G., Peethambaram, S. and Castella, J.C. 2011. Comparison of three maps at multiple resolutions: a case study of land change simulation in Cho Don District, Vietnam. *Annals of the Association of American Geographers* 101(1): 45-62. doi:10.1080/00045608.2010.517742.

Ramalingan, S., Liu, Z-Q. and Iourinski, D. 2006. Curvature-Based Fuzzy Surface Classification. *IEEE Transactions on Fuzzy Systems* 14(4): 573-589.

Satty, T.L. and Vargas, L.G. 2001. Models, methods, concepts and applications of the analytic hierarchy process. *International Series in Operations Research and Management Science* 34b:1–352.

Shahabi, H., Ahmad, B.A., Ahmad, B.B., Amiri, M.J.T., Keihanfard, S. and Ebrahimi, S. 2016. Assessment of WLC and Fuzzy Logic Methods for Site Selection of Water Reservoirs in Malaysia. *Polish Journal of Environmental Studies* 25(3): 1223-1231.

Skole, D.L. 1994. Data on global land-cover change: acquisition, assessment, and analysis. In: W. B. Meyer, B.L. Turner II (eds), *Changes in Land Use and Land Cover: A Global Perspective*. Cambridge: Cambridge University Press, pp.437 –471.

Stéphenne, N. and Lambin, E.F. 2001. A dynamic simulation model of land-use changes in Sudano-Sahelian countries of Africa (SALU). *Agriculture, Ecosystems and Environment* 85: 145–161.

Tagil, S. and Jenness, J. 2008. GIS-Based Automated Landform Classification and Topographic, Landcover and Geologic Attributes of Landforms

Around the Yazoren Polje, Turkey. *Journal of Applied Sciences* 8: 910–921.

Tajbakhsh, S.M., Memarian, H., Moradi, K.,and Afshar, A.H.A. 2018. Performance comparison of land change modeling techniques for land use projection of arid watersheds. *Global Journal of Environmental Science and Management* 4(3): 263-280.

Tayyebi, A., Delavar, M.R., Yazdanpanah, M.J., Pijanowski, B.C., Saeedi, S. and Tayyebi, A.H. 2010. A spatial logistic regression model for simulating land use patterns: A case study of the Shiraz Metropolitan Area of Iran. In: Chuvieco et al. (eds.), *Advances in Earth Observation of Global Change,* doi: 10.1007/978-90-481-9085-0_3.

Thomas, H. and Laurence, H.M. 2006. Modeling and projecting land-use and land-cover changes with a cellular automaton in considering landscape trajectories: An improvement for simulation of plausible future states. *EARSeLeProc* 5: 63–76.

Thomas, M. 2012. A geomorphological approach to geodiversity - Its applications to geoconservation and geotourism. *Quaestiones Geographicae* 31: 81–89.

Tian, G.J., Ouyang, Y., Quan, Q.A. and Wu, J.G. 2011. Simulating spatiotemporal dynamics of urbanization with multi-agent systems – A case study of the Phoenix metropolitan region, USA. *Ecological Modelling* 222: 1129-1138.

Tunçay, T., Bayramin, I., Öztürk, H.S., Kibar, M. and Başkan, O. 2014. The use of remote sensing and geographic information system techniques to determine relationships between land use and landform. *Toprak Su Dergisi* 3(2): 124-136.

Verburg, P.H., Schot, P., Dijst, M. and Veldkamp, A. 2004. Land use change modeling: current practice and research priorities. *GeoJournal* 61: 309–324.

Verburg, P.H., van de Steeg, J., Veldkamp, A. and Willemen, L. 2009. From land cover change to land function dynamics: A major challenge to improve land characterization. *Journal of Environmental Management* 90: 1327–1335.

Verburg, P.H., Veldkamp, W.S.A., Espaldon, R.L.V. and Mastura, S.S.A. 2002. Modeling the spatial dynamics of regional land use: The CLUE-S model. *Environmental Management* 30(3): 391–405.

Vitousek, P.M. 1994. Beyond global warming: ecology and global change. *Ecology* 75: 1861 – 1876.

Wang, H., Li, X.B., Long, H.L., Qiao, Y.W. and Li, Y. 2011. Development and application of a simulation model for changes in land-use patterns under drought scenarios. *Computers & Geosciences* 37: 831-843.

Weiss, A.D. 2000. Topographic position and landforms analysis. Poster, http://www.jennessent.com/downloads/tpi-poster-tnc_18x22.pdf.

Weiss, A.D. 2005. Topographic Position and Landforms Analysis. *Ecoregional Data Management Team the Nature Conservancy* 4343–4345.

Wilson, J.P. and Gallant, J.C. 2000. Primary Topographic Attributes. In: Wilson, J.P. and Gallant, J.C. (eds), *Terrain Analysis: Principles and Applications.* John Wiley & Sons p.51-85.

Yang, X., Zheng, X.Q. and Chen, R. 2014. A land use change model: Integrating landscape pattern indexes and Markov-CA. *Ecological Modelling* 283: 1-7.

Yang, X., Zheng, X.Q. and Lv, L.N. 2012. A spatiotemporal model of land-use change based on ant colony optimization, Markov chain, and cellular automata. *Ecological Modelling* 233: 11–19.

Yeganeh, N. and Sabri, S. 2014. Flood vulnerability assessment in Iskandar Malaysia using multi-criteria evaluation and fuzzy logic. *Research Journal of Applied Sciences, Engineering and Technology* 8(16): 1794-1806.

Yulianto, F., Maulana, T. and Khomarudin, M.R. 2018. Analysis of the dynamics of land use change and its prediction based on the integration of remotely sensed data and CA-Markov model, in the upstream Citarum Watershed, West Java, Indonesia. *International Journal of Digital Earth* 2018, doi: 10.1080/17538947.2018.1497098.

Yulianto, F., Prasasti, I., Pasaribu, J.M., Fitriana, H.L., Zylshal, Haryani, N.S. and Sofan, P. 2016. The dynamics of land-use/land cover change modeling and their implication for the flood damage assessment in the Tondano watershed, North Sulawesi, Indonesia. *Modeling Earth System and Environment* 2: 47, doi: 10.1007/s40808-016-0100-3.

Yulianto, F., Suwarsono and Sofan, P. 2016. The utilization of remotely sensed data to analyze the estimated volume of pyroclastic deposits and morphological changes caused by the 2010–2015 eruption of Sinabung volcano, North Sumatra, Indonesia. *Pure and Applied. Geophysics* 173: 2711-2725.